JOURNAL OF COMPUTATIONAL PHYSICS 9, 237–253 (1972)

An Inverse Solution Procedure for Turbulent Swirling Boundary Layer Combustion Flow

D. G. LILLEY* AND N. A. CHIGIER†

Department of Chemical Engineering and Fuel Technology, The University, Sheffield S1 3JD, England

Received July 23, 1970

A detailed description is presented of the mathematical and computational aspects of the general inverse solution procedure developed for turbulent swirling boundary layer combustion flow. The situation is that a nonrecirculating swirling turbulent flame in which experimental time-mean measurements of the axial and swirl velocities v_z and v_θ, temperature T and chemical species concentrations m_j have been made. The problem is to calculate the distributions of the significant turbulent momentum, enthalpy and chemical species' flux components (τ_{rz}, $\tau_{r\theta}$, $(J_h)_r$ and $(J_j)_r$) and associated exchange coefficients, Prandtl and Schmidt numbers. A solution is provided by the inverse solution TEXCO code; it provides a link between mean measurements and certain correlations of turbulent fluctuation components and throws light on the appropriateness or otherwise of any given turbulence model for the flow under consideration.

The method is applied to both isothermal and chemically reacting flows, and calculations show that previous assumptions of isotropy of the turbulent stress tensor and constancy of Prandtl–Schmidt numbers are not generally valid. The exchange coefficients are shown to be functions of the degree of swirl and position in the flowfield. For the isothermal case, it is shown that the assumption of an isotropic uniform mixing length parameter distribution is quite feasible for weak swirl but is progressively less valid as the degree of swirl increases. For the flame case, similar results are obtained and the turbulent viscosity is found to be highly nonisotropic.

INTRODUCTION

Many research experiments are being conducted which concern time-mean measurements on quasi-steady turbulent combustion systems. Analysis of the results can lead to knowledge of fundamental mixing and chemical-kinetic processes and provide hypotheses about the process. On the other hand, solution of the Reynolds equations for time-mean values is restricted through lack of

* Now at Department of Mathematics and Computing Science, The Polytechnic, Sheffield S1 1WB, England.

† On leave of absence, 1970–71, at Ames Research Center, NASA, Moffett Field, CA, 94035.

knowledge of suitable turbulence hypotheses and experimental verification is required of models and predicted mean flow patterns. Comparison of time-mean predictions and time-mean measurements could suggest improvements to turbulence models.

Here, consideration is given to an alternative simpler approach for the special case of nonrecirculating swirling flames. An analytical method has been devised for calculating certain components of the turbulent fluxes and associated exchange coefficients directly from limited experimental time-mean data, without the need for a complete solution to the problem [1]. It is an intermediate step which has been used on both swirling isothermal [2] and combustion [3] systems. The method allows distributions, of τ_{rz}, $\tau_{r\theta}$, $(J_h)_r$ and $(J_j)_r$ (the significant flux components) and associated exchange coefficients to be determined from experimental mean distributions of v_z, v_θ, T and m_j. It thus throws light on the appropriateness or otherwise of any given turbulence model for the flow under consideration.

This paper contains four sections concerned with the basic equations and assumptions, the calculation procedure, the computer program and results obtained for both isothermal and flame jet systems with swirl.

Basic Equations and Assumptions

Basic Differential Equations

The basic turbulent flux equations of conservation of mass, momentum, enthalpy, and chemical species are assumed to hold for the time-mean variables with only the turbulent contributions to the fluxes (the molecular contributions being negligibly small in fully turbulent free flow). They are written in a cylindrical polar coordinate system (z, r, θ) and the motion is assumed to be quasi-steady ($\partial/\partial t = 0$) and axisymmetric ($\partial/\partial\theta = 0$) with no external force. Invoking boundary layer assumptions and neglecting kinetic heating, they become [4]

$$r\left[\rho\left(v_z\frac{\partial v_z}{\partial z} + v_z\frac{\partial v_z}{\partial r}\right) + \frac{\partial p}{\partial z}\right] = \frac{\partial}{\partial z}(r\tau_{rz}), \tag{1}$$

$$r^2\rho\left(v_z\frac{\partial v_\theta}{\partial z} + v_r\frac{\partial v_\theta}{\partial r} + \frac{v_r v_\theta}{r}\right) = \frac{\partial}{\partial r}(r^2\tau_{r\theta}), \tag{2}$$

$$r\rho\left(v_z\frac{\partial h}{\partial z} + v_r\frac{\partial h}{\partial r}\right) = -\frac{\partial}{\partial r}[r(J_h)_r], \tag{3}$$

$$r\left[\rho\left(v_z\frac{\partial m_j}{\partial z} + v_r\frac{\partial m_j}{\partial r}\right) - R_j\right] = -\frac{\partial}{\partial r}[r(J_j)_r], \tag{4}$$

$$\frac{\partial}{\partial z}(\rho v_z) + \frac{1}{r}\frac{\partial}{\partial r}(r\rho v_r) = 0, \tag{5}$$

$$\rho \frac{v_\theta^2}{r} = \frac{\partial p}{\partial r}, \tag{6}$$

There is an equation of type (4) for each chemical species present.

With these assumptions is the implication that there be no recirculation; thus flames to which the subsequent work is applicable must have sufficiently high Reynolds numbers and low degrees of swirl so as not to invalidate the assumptions. The method is applicable, however, downstream of a recirculation zone.

If experimental mean measurements of v_z, v_θ, T and m_j are available and τ_{rz}, $\tau_{r\theta}$, $(J_h)_r$ and $(J_j)_r$ are considered as unknowns, the equation system (1-6) is not closed. Further unknowns are v_r, ρ, p, h and R_j which leads to $(2 + n)$ excess unknowns, where n is the number of chemical species present.

Thermodynamic Relationships

Thermodynamic relationships provide the necessary extra equations to close the system; these equations are taken as

$$p = \rho \frac{R}{M} T, \tag{7}$$

$$h = c_p T + \sum_j (H_j m_j), \tag{8}$$

$$R_j = -F_j \exp(-E_j/RT). \tag{9}$$

There are n equations of type (9). Equation (7) is the ideal equation of state and density variations are determined from temperature variations under the assumption that chemical composition has negligible effect on density and that pressure changes are caused solely through Eq. (6). Equation (8) demands that an average specific heat c_p be used for the mixture and that its value be independent of temperature. The rates of production R_j of chemical species j are usually provided by expressions of the Arrhenius type (9), where F_j, the frequency (preexponential) factor, and E_j, the activation energy, are used. One fewer chemical species' differential equations of type (4) and one fewer rate equations of type (9) need be considered since the relation

$$\sum_j m_j = 1 \tag{10}$$

is always applicable.

More realistic thermodynamic simulations then provided here have been used [4] and, if accuracy demands using them, their incorporation into the program is straightforward.

Flux Laws

It may be shown that the turbulent fluxes are related to correlations of turbulent fluctuations, measured in hot-wire anemometry, by the relations (neglecting the density fluctuation contributions)

$$\tau_{rz} = -\rho\overline{v_r' v_z'}, \qquad \tau_{r\theta} = -\rho\overline{v_r' v_\theta'}, \tag{11}$$

$$(J_h)_r = \rho\overline{v_r' h'}, \qquad (J_j)_r = \rho\overline{v_r' m_j'}. \tag{12}$$

By analogy with laminar flows extensions of Newton's constitutive stress–strain relation, Fourier's law of heat conduction and Fick's law of diffusion have been postulated and used in the past with variable turbulent exchange coefficients μ, Γ_h, and Γ_j. For the nonisotropic model used here these extensions are taken as

$$\tau_{rz} = \mu_{rz}\frac{\partial v_z}{\partial r}, \qquad \tau_{r\theta} = \mu_{r\theta r}\frac{\partial}{\partial r}(v_\theta/r), \tag{13}$$

$$(J_h)_r = -(\Gamma_h)_r\frac{\partial h}{\partial r}, \qquad (J_j)_r = -(\Gamma_j)_r\frac{\partial m_j}{\partial r}. \tag{14}$$

Conversely to the prediction methods which require specification of the exchange coefficients as inputs, these values are the output of the method described here. A check on their values, spatial distributions, constancy, isotropy and determination via a turbulence model is the main use of the subsequent program to which experimental mean data are the input.

Turbulence Models

It is the unknown flux components which lead to difficulties in satisfactorily solving the Reynolds equations for time-mean values. Predictions can only be made if they are specified in terms of mean quantities or in terms of further unknowns with correspondingly further equations.

A turbulence model is some hypothesis which specifies the unknown fluxes and so closes the system and allows Eqs. (1)–(6) and (7)–(9) to be solved for time mean $\underline{v}$, h, T, m_j, p and ρ. This can take the form of specifying the fluxes directly or indirectly by way of the exchange coefficients.

For the nonrecirculating flow system here, consideration will be given only to extensions of Prandtl's mixing length hypothesis [5]. It is assumed that the primary viscosity component μ_{rz} can be specified in terms of local mean conditions via a

mixing length l_{rz} and a mixing length parameter λ_{rz}. The relation may take the form

$$\mu_{rz} = \rho l_{rz}^2 \left[\left(\frac{\partial v_z}{\partial r} \right)^2 + \left(r \frac{\partial}{\partial r} (v_\theta / r) \right)^2 \right]^{1/2}, \tag{15}$$

or

$$\mu_{rz} = \rho l_{rz}^2 \left| \frac{\partial v_z}{\partial r} \right|, \tag{16}$$

together with

$$l_{rz} = \lambda_{rz} \cdot r_{\max} . \tag{17}$$

The other exchange coefficients are related to μ_{rz} via Prandtl, Schmidt and $r\theta$-viscosity numbers defined by

$$\sigma_h = \mu_{rz}/(\Gamma_h)_r , \qquad \sigma_j = \mu_{rz}/(\Gamma_j)_r , \qquad \sigma_{r\theta} = \mu_{rz}/\mu_{r\theta} . \tag{18}$$

Calculation Method

Results of experimental time-mean measurements are assumed to be in the form of algebraic curves, obtained by fits to the experimental data. Calculation of the unknown turbulent fluxes requires differentiation and integration operations to be performed on these fitted curves. The curves are rarely of a simple form and analytic handling, though straightforward, is somewhat involved. The most serious drawback of an analytic method, though, would be lack of generality—different algebraic forms of the fitted curves from different experimental investigations would necessitate revised mathematical work before quantitative computations could be performed.

Rather than use a limited analytic method, the authors preferred to develop a direct numerical technique in the form of a generally applicable computer program, requiring only the setting of controls and specification of the fitted curves at appropriate places. Prime factors during the development were accuracy, economy, generality, and simplicity of operation, the intention being that experimentalists primarily interested in using the program, without concerning themselves greatly with the computational details, could do so with a minimum of effort.

Numerical Analysis

Finite difference simulations of the differential Eqs. (1)–(6) are required. Standard numerical formulas [6] are used for differentiation and integration of any given function $y = y(x)$.

For differentiation a three-, five-, or seven-point central difference formula [6] is used over a series of points $x_{-3}, x_{-2}, \ldots, x_3$ with constant x-interval h; it is obtained from

$$hy_0' = \left(\mu\delta - \frac{1}{6}\mu\delta^3 + \frac{1}{30}\mu\delta^5 \cdots\right) y_0, \tag{19}$$

where

$$\mu(\phi_i) = \tfrac{1}{2}(\phi_{i+1/2} + \phi_{i-1/2}) = \text{averaging operator},$$

$$\delta(\phi_i) = \phi_{i+1/2} - \phi_{i-1/2} = \text{central difference operator},$$

$$h = x_{i+1} - x_i = \text{constant } x\text{-interval between nodes.}$$

Truncation of formula (19) after the first, second, or third term yields the three-, five-, or seven-point central difference formulas

$$y_0' = \frac{y_1 - y_{-1}}{2h} + o(h^2), \tag{20}$$

$$y_0' = \frac{1}{12h}[-y_2 + 8y_1 - 8y_{-1} + y_{-2}] + o(h^4), \tag{21}$$

$$y_0' = \frac{1}{60h}[y_3 - 9y_2 + 45y_1 - 45y_{-1} + 9y_{-2} - y_{-3}] + o(h^6). \tag{22}$$

Here $y_i = y(x_i) = y(x + ih)$.

Integrations are performed using either the trapezoidal or Simpsons's rule. The trapezoidal rule is obtained by expressing the integrand in terms of central differences via

$$\begin{aligned}\int_{x_0}^{x_n} y\,dx &= h\left[\left(\frac{1}{2}y_0 + y_1 + y_2 + \cdots + y_{n-1} + \frac{1}{2}y_n\right)\right.\\ &\quad \left. - \frac{1}{12}(\mu\delta y_n - \mu\delta y_0) + \frac{11}{720}(\mu\delta^3 y_n - \mu\delta^3 y_0)\right]\\ &= \frac{h}{2}[(y_0 + y_n) + 2(y_1 + y_2 + \cdots + y_{n-1})] + o(h^3),\end{aligned} \tag{23}$$

where $y_i = y(x_i) = y(x + ih)$.

Simpson's rule is far more accurate and obtained by expressing the integral over two adjoining intervals in terms of central differences at the central pivotal point, viz.,

$$\begin{aligned}\frac{1}{2h}\int_{x_{-1}}^{x_1} y\,dx &= \left(1 + \frac{1}{6}\delta^2 - \frac{1}{180}\delta^4 + \cdots\right) y_0\\ &= y_0 + \frac{1}{6}(y_1 - 2y_0 + y_{-1}) + o(h^4),\end{aligned}$$

and hence

$$\int_{x_{-1}}^{x_1} y\,dx = \frac{h}{3}(y_{-1} + 4y_0 + y_1) + o(h^5),$$

and

$$\int_{x_0}^{x_{2n}} y\,dx = \frac{h}{3}[(y_0 + y_{2n}) + 4(y_1 + y_3 + \cdots + y_{2n-1}) + 2(y_2 + y_4 + \cdots + y_{2n-2})] + o(h^5). \tag{24}$$

Any other integration or differentiation formulas can be used. However, there is no difficulty with regard to stability, convergency or accuracy of the above formulas, since they are used on smooth experimentally-fitted curves which are "well behaved", in the sense that higher-order differences tend to zero as the order of the difference increases. In the program used by the authors [1, 4] all derivatives are calculated by use of the seven-point formula [Eq. (22)] and most integrals by Simpson's rule [Eq. (24)]. Provided care is taken with choice of the mesh over which the multipoint formulas are used, final results obtained will be in no way inferior to those obtained analytically.

Grid System[1]

Figure 1 shows the grid system in use at any particular axial station z. It is defined by δz and NPT, the number of J values. The position $J = NPT$ is preselected to be just beyond the region of interest, at a point with radial coordinate $r_{\text{edge}} = \xi_{\text{edge}} \cdot (z + a)$, chosen where for instance $u/u_m \leqslant 0.01$. Dividing r_{edge} by $6 \cdot NPT$ gives the δr value between successive K lines. Thus there are six δr divisions between successive J lines and so the K values repeat themselves $(NPT - 1)$ times. The bijective mapping

$$(I, J, K) \leftrightarrow (z + (I - 4)\,\delta z, (6J + K - 7)\,\delta r) \tag{25}$$

shows that the 3-tuple (I, J, K) $(1 \leqslant I \leqslant 7, 1 \leqslant J \leqslant NPT, 1 \leqslant K \leqslant 6)$ defines uniquely the $42 \cdot NPT$ nodes associated with this axial station z and vice versa. The K range is extended to 7 via the equation $(I, J, 7) = (I, J + 1, 1)$ for later convenience.

[1] A 3-tuple subscripting system (I, J, K) is employed here which differs slightly from the simpler 2-tuple system (I, J) previously described [2, 3]. The previous I and J correspond directly with the present I and K, and define the 7×7 subgrid around each J-point P; see Figs. 1 and 2. The subscript J now denotes to which radial point P the subgrid refers and enables the discussion of integration across the layer to be more complete and interesting points P to be stated explicitly (for example, those points P with J odd at which Simpson integration reaches a temporary halt). This 3-tuple system is used in [1, 4] where further use is made of the J parameter.

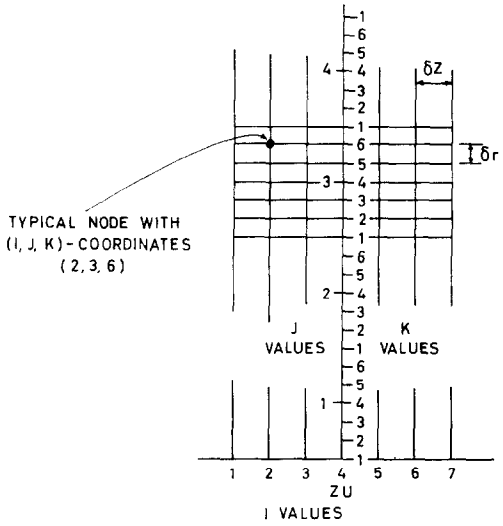

FIG. 1. The grid system for each axial station ZU.

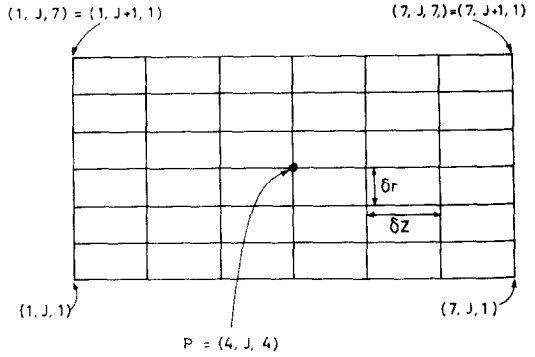

FIG. 2. The subgrid associated with points $P = (4, J, 4)(1 \leqslant J \leqslant NPT)$.

The points P with (I, J, K)-coordinates $(4, J, 4)$ $(1 \leqslant J \leqslant NPT)$ deserve special mention and are shown in Fig. 2, together with their surrounding small 7×7 rectangular subgrid. For it is at these points that the left hand sides of Eqs. (1)–(4) are to be calculated.

More noteworthy perhaps are those points P with J odd; that is the set $\{(4, J, 4)(1 \leqslant J \leqslant NPT, J \text{ odd})\}$. For it is these points at which the Simpson rule integration of the left hand sides reaches a temporary halt after its three-point application over the points $(4, J - 2, 4)$, $(4, J - 1, 4)$ and $(4, J, 4)$ with $h = 6 \cdot \delta r$.

Output may be effected at these points together with exchange coefficient calculations from the fluxes.

Calculation Procedure

Assume that curves have been fitted to experimentally observed time-mean axial and swirl velocities, v_z and v_θ, temperature T and chemical species' concentrations m_j. Thus for a given degree of swirl S, axial distance z and radial distance r, their values are easily calculated. The only unknowns in the equation system (1)–(6) are ρ, p, v_r, τ_{rz}, $\tau_{r\theta}$, $(J_h)_r$ and $(J_j)_r$, when the thermodynamic relations are assumed. These can now be calculated at all points P of the flowfield, which are in the set $\{(4, J, 4)(1 \leqslant J \leqslant NPT, J \text{ odd})\}$ for some choice of axial station z and number of J values NPT.

In order to allow the outward sweep calculation, as mentioned above, the axis subpressures at the nodes $(I, 1, 1)(1 \leqslant I \leqslant 7)$ are first calculated from Eq. (6) by inward integration using the trapezoidal rule [Eq. (23)] with $h = \delta r$. Density changes due to pressure differences caused via Eq. (6) are ignored in this calculation, since the variation in pressure is small. The use of calculating p is to establish $\partial p/\partial z$ for Eq. (1) which may not be small compared with the other terms in that equation.

Let P be one of the points $(4, J, 4)$ at the center of a small 7×7 rectangular subgrid. Since values of v_z, v_θ, T and m_j [and hence h from Eq. (8) and ρv_z] are easily obtained at any of the nodes (I, J, K) $(1 \leqslant I, K \leqslant 7)$, axial and radial derivatives of these are immediately calculable [using the seven-point formula Eq. (22), for example] at the nodes $(4, J, K)$ $(1 \leqslant K \leqslant 7)$ and $(I, J, 4)$ $(1 \leqslant I \leqslant 7)$, respectively. Not all of these are required and thus not all of them are calculated. Most are calculated only at the center node $(4, J, 4)$, the axial derivative of ρv_z being the only exception, being required at the nodes $(4, J, K)$ $(1 \leqslant K \leqslant 7)$. The reason for this exception is so that a better calculation of v_r can be made, using Simpson integration of Eq. (5) between the nodes $(4, J, K)$ $(1 \leqslant K \leqslant 7)$ taking $h = \delta r$.

The procedure for calculating the unknowns successively at P (the node $(4, J, 4)$ (J fixed)) is as follows:

(i) The density ρ is calculated at the nodes (I, J, K) $(1 \leqslant I, K \leqslant 7)$ from Eq. (7) from a knowledge of T at these nodes and disregard of density change due to pressure. Hence ρv_z is calculated at these nodes and $(\partial/\partial z)(\rho v_z)$ at $(4, J, K)$ $(1 \leqslant K \leqslant 7)$.

(ii) The pressure p is calculated at the nodes (I, J, K) $(1 \leqslant I, K \leqslant 7)$ from Eq. (6) by outward trapezoidal integration with $h = \delta r$, using the axis subpressures as boundary conditions. This exactly reverses the initial axis subpressure calculation. Hence $\partial p/\partial z$ is obtained at P.

(iii) The radial velocity v_r is calculated at P from Eq. (5) using outward Simpson integration with $h = \delta r$.

(iv) The values of all terms on the left hand sides of Eqs. (1)-(4) are calculated at P and values appropriate to the right hand sides are deduced.

(v) If J is odd and greater than unity, Simpson integration of these values over the three points $(4, J-2, 4)$, $(4, J-1, 4)$, and $(4, J, 4)$ with $h = 6 \cdot \delta r$, together with values of $r\tau_{rz}$, $r^2\tau_{r\theta}$, $r(J_h)_r$ and $r(J_j)_r$ at $(4, J-2, 4)$, enables the fluxes τ_{rz}, $\tau_{r\theta}$, $(J_h)_r$, and $(J_j)_r$ to be calculated at $(4, J, 4)$. If J is unity or even, the values of the right hand sides are stored and no integration is performed until the next odd J value is reached.

(vi) If J is odd and output is required here, calculation and output are made of the fluxes, exchange coefficients, Prandtl, Schmidt and $r\theta$-viscosity numbers and mixing length parameter.

Repetition of this process for higher values of J allows cross-stream results at some axial station to be deduced If experimental mean measurements of p and/or v_r are available, step (ii) and/or (iii) may be omitted. Boundary conditions are required for the integration stages; these are

$$p = p_\infty \quad \text{at} \quad r = \infty, \tag{26}$$

$$v_r = \tau_{rz} = \tau_{r\theta} = (J_h)_r = (J_j)_r = 0 \quad \text{at} \quad r = 0. \tag{27}$$

Repetition of the procedure at other axial stations z and other swirl numbers S enables full spatial and swirl distributions to be obtained.

The TEXCO Computer Program

The program described and listed in [1, 4] is equipped with a simplified combustion model but modification to more complete models is straightforward. Consideration is given to the degenerate case of a simple chemical reaction of the form

$$1 \text{ kg} \cdot \text{fuel} + i \text{ kg} \cdot \text{oxidant} \rightarrow (1 + i) \text{ kg} \cdot \text{products}, \tag{28}$$

where combustion is assumed to occur in a single step between just two chemical species, fuel and oxidant. Equation (8) now simplifies to

$$h = c_p \cdot T + H_{fu} \cdot m_{fu}, \tag{29}$$

and enables the enthalpy equation to be solved for Prandtl numbers if m_{fu} is known. Schmidt numbers are obtained from Eq. (4) with $j = fu$. Thus specification of the distribution of but one chemical species' concentration, fuel, enables the full generality of the method to be outlined.

The TEXCO program has been written (in Fortran IV) primarily with a view to maximizing ease of use and accuracy, perhaps at the expense of computer time. Full details of the organization of the computer program, together with the general listing, are available in [1, 4].

Ease of use is achieved by limiting to the MAIN subprogram those features which characterize the particular flow configuration being solved. Accuracy is enhanced by having in-built into the general subroutine CALC (which performs the series of calculations (i)–(vi) above, storage and output) seven-point central difference differentiation formulas [Eq. (22)] and three-point Simpson's rule integration formulas [Eq. (24)]. These possess local accuracy of order h^6 and h^5, respectively. The CALC routine is quite general in comparison to MAIN.

The one remaining subroutine PLOT is used only when quick scenic output is required in the form of lineprinter graph plots. Modifications only with regard to scaling may be necessary, but further storage and different types of print could easily be incorporated so as to provide very detailed plots.

Generally a user's attention is restricted to MAIN and its breakdown into chapters simplifies his task. MAIN differs for each flow configuration and reliable distributions must be used and entered correctly. If several chemical species' concentrations have been measured further equations of type (4) and reaction rates (9) must be included.

With regard to accuracy and economy, decisions on the size of mesh and checks on the variation of results at a particular spatial position may be made by their independent variation. Generally, with the high accuracy seven-point central difference derivative formula, the calculations are almost independent of the size of grid in the z-direction if "smooth" experimentally fitted data curves are used; however, the cross-stream integrations are somewhat dependent on the number of points across the layer as expected. A value of about 150 points across a particular mixing region has been found to be quite adequate. A three-, five-, or seven-point differentiation formula may be used and the grid-size and variable dimensions may be cut down accordingly.

Application of the Method

Results are presented and discussed of the application of the TEXCO code to some of the very limited experimental data on turbulent swirling flows: the isothermal swirling jet and the swirling flame. The values of all quantities calculated here are directly dependent upon the accuracy of the experiments, the curve fitting and the calculation procedure. Accuracy checks were made with the calculation procedure by varying the size of grid and number of points NPT across the mixing layer. Since the calculation is a Simpson integration across the mixing layer,

with ordinate values calculated each time from the experimental curves, decreasing the size of the grid and increasing NPT can increase almost without limit the accuracy of the calculation. It is considered that mesh parameters making the calculation procedure extremely accurate have been used and that sufficient care has been taken in the other procedures for all the conclusions to be valid and the magnitude of calculated terms to have an accuracy of ten per cent.

The Isothermal Swirling Jet

The results presented and discussed refer to predictions made from experimental mean data of Chigier and Chervinsky [7], who conducted an experimental study of isothermal turbulent jets with degrees of swirl S from 0.0 to 0.6.

In [7] curves were fitted through the experimental points of time-mean velocities and pressure and a set of equations with empirical constants were given so that their variations with position and degree of swirl were readily calculable.

Since the study concerned itself with isothermal mixing of a jet of the same fluid as the surroundings, the enthalpy and species equations [Eqs. (3) and (4)] could be dispensed with and the program operated with only two different equations, for τ_{rz} and $\tau_{r\theta}$. Results show [2, 4], that τ_{rz} and μ_{rz} are, in general, of larger magnitude than $\tau_{r\theta}$ and $\mu_{r\theta}$, τ_{rz} and μ_{rz} both increasing with swirl in the initial region near the orifice but decreasing with swirl in the fully developed region. The $r\theta$-viscosity number $\sigma_{r\theta}$ is generally greater than unity and progressively so as the degree of swirl increases, the deviation from unity being more pronounced in the initial region.

Mixing length parameters calculated according to Eq. (15) and similar for $\lambda_{r\theta}$ are shown in Fig. 3 for the initial and fully developed regions. There was little downstream variation after the first five diameters. For nonswirling jets it has been found that good predictions of mean velocity distributions can be made with the assumption that λ_{rz} is constant and equal to 0.0845; see [8]. An examination of Fig. 3 shows that there is a variation of both λ_{rz} and $\lambda_{r\theta}$ with spatial position and degree of swirl. The spatial variations of λ_{rz} are seen to be greater for swirling than for nonswirling jets, but spatial variations of $\lambda_{r\theta}$ are very small. The increase in λ_{rz} towards the center shows that predictions using a constant mixing length predict too low an effective viscosity μ_{rz}, and hence a distribution of u/u_m which is too pointed near $\xi = 0$. On the basis of the results shown in Fig. 3 it may be concluded that good predictions can be made for weakly swirling jets with the assumption that λ_{rz} and $\lambda_{r\theta}$ are both equal to 0.1, whereas for higher degrees of swirl a smaller value of $\lambda_{r\theta}$ is appropriate. Thus, despite the effective viscosity being nonisotropic and nonuniform, a mixing length parameter distribution which is isotropic and uniform is quite feasible for weakly swirling jets, but is progressively less valid as the degree of swirl increases.

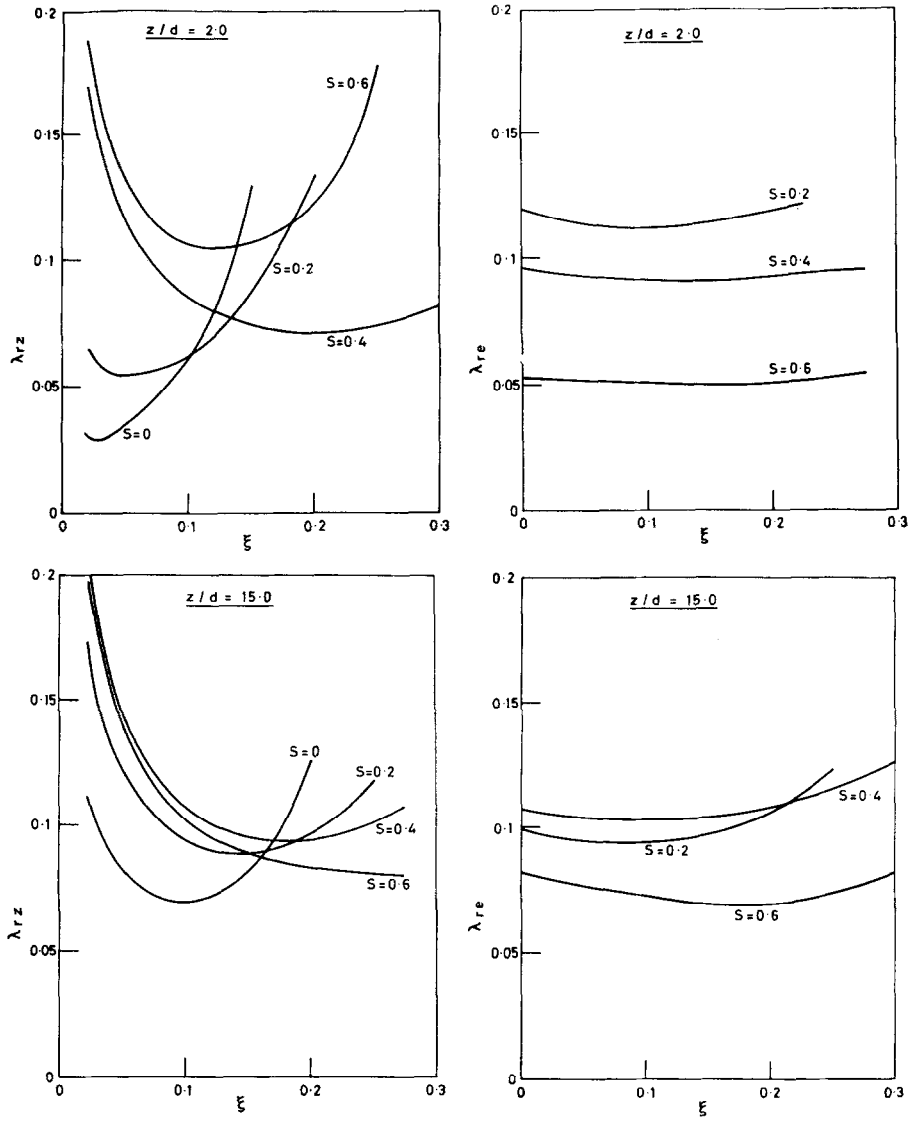

FIG. 3. Radial distributions of mixing length parameters λ_{rz} and $\lambda_{r\theta}$ in the initial and fully developed regions in isothermal regions.

The Swirling Flame

This section deals with the case of free swirling jet flames with combustion of fuel gas. The calculation procedure is extended to calculate turbulent viscosity, Prandtl and Schmidt numbers from experimental mean data of velocity, temperature and concentration in turbulent flames, for a limited range of degrees of swirl.

Owing to the lack of experimental results reported of spatial distributions of mean values, the method in its full generality cannot yet be used. Up to now there appears to be no reported results on concentration measurements in turbulent swirling flames and thus it would be disproportionate to solve equations of type (4) for Schmidt numbers. But Prandtl numbers may still be obtanied via a simplified model.

The degenerate case of a simple chemical reaction, as previously described, is considered and the enthalpy equation can be solved for Prandtl numbers if m_{fu} is known. On the basis of concentration measurements of Hawthorne [9] and the velocity measurements of Chigier [10] it has been assumed that the Schmidt number for the fuel concentration within the flame boundary is the same as for an isothermal jet, i.e., 0.7. Extending this to the case of a swirling flame yields the result that, within the flame, concentration distribution can be obtained from the measured mean velocities of each flame, which differ according to the degree of swirl. To complete the fuel distribution, zero concentration is assumed outside the flame boundary, which is taken to be the radial position of maximum temperature at a given axial station.

The results presented and discussion refer to predictions made from experimental time-mean data of Chigier and Chervinsky [10] who conducted an experimental study of turbulent swirling flames with degrees of swirl S from 0.0 to 0.2. The flames were premixed (about 20 % fuel) and variations of specific heat and density because of composition were ignored in the calculations; data appropriate to air were used for c_p and p.

The distributions of the rz- and $r\theta$-components of τ and μ are found to be very similar to the isothermal case. The nonisotropy was even more marked and all components decrease progressively with swirl at this downstream position; the experimental results did not extend to the initial region.

Figures 4 and 5 show distributions of turbulent Prandtl and $r\theta$-viscosity numbers in flames. In general, the Prandtl number increases with swirl, radial and axial increases, except for the region near the axis where in any case gradients are small. These variations are not in agreement with the accepted constant value near 0.7. A lack of experimental measurements of the swirl velocity radial distribution necessitated the use of an approximate v_θ-distribution and hence only qualitative values of $\mu_{r\theta}$ and $\sigma_{r\theta}$ could be calculated. In particular, their values were indeterminate in the near zero $r\theta$-strain of the almost solid body rotation in the central

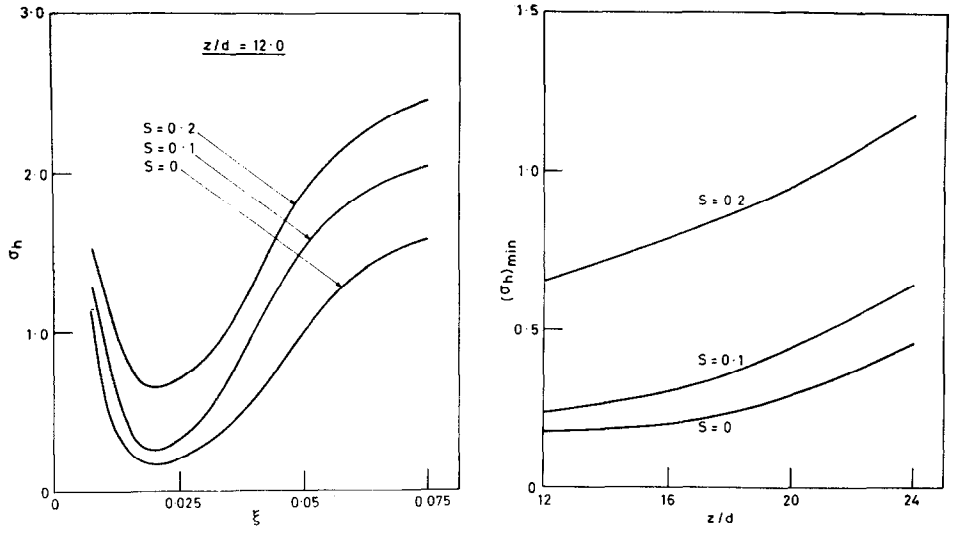

FIG. 4. Distribution of turbulent Prandtl number in flames.

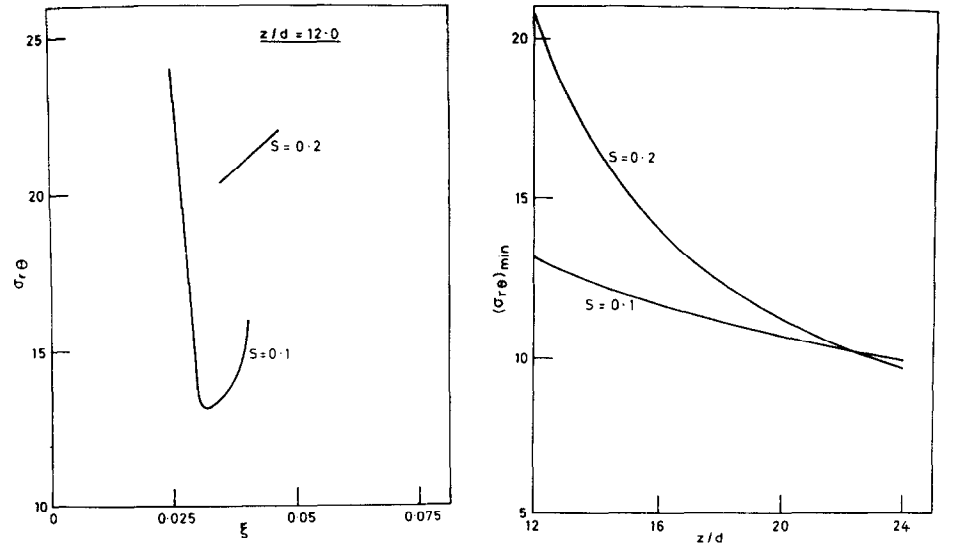

FIG. 5. Distribution of $r\theta$-viscosity number in flames.

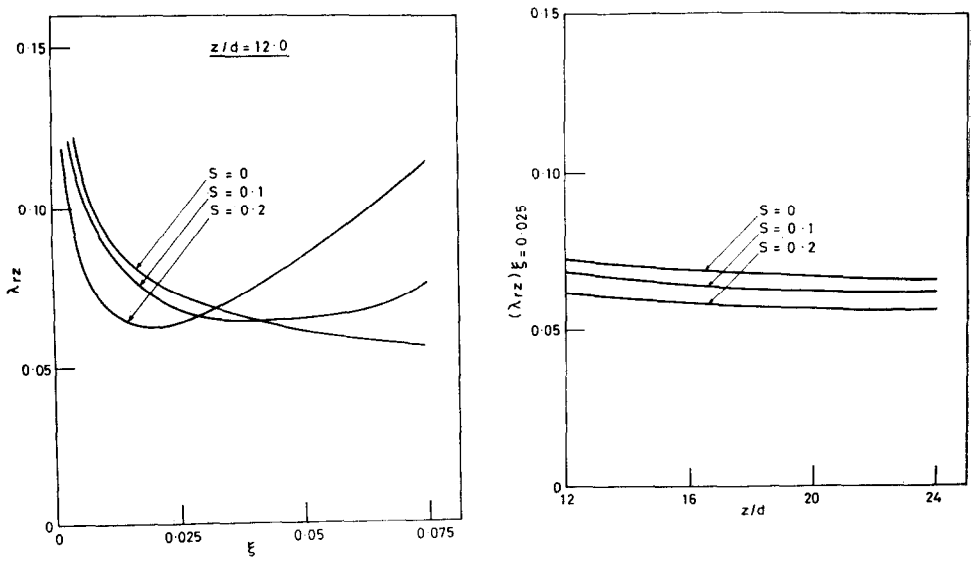

FIG. 6. Distribution of mixing length parameter λ_{rz} in flames.

core region. Values of $\sigma_{r\theta}$ in the outer region are shown; they were found to be quite large whereas in the isothermal case they were of order unity. The explanation could be the limited data or the influence of the discontinuities at the flame boundary.

Mixing length parameters λ_{rz} and $\lambda_{r\theta}$ have been calculated using Eq. (15) and the distribution of λ_{rz} is shown in Fig. 6. The rz-value may be compared with the accepted nonreacting nonswirling value of between 0.075 and 0.09; the $r\theta$-values are not shown since these were consistently small (about 0.02) and are not useful since $r\theta$-viscosity number distributions have been given. It can be seen that λ_{rz} varies little with swirl or axial position; indeed the only variation of interest was that with ξ. Even then the higher values near the axis contribute little, since gradients are small here. The downstream variation shown of λ_{rz} calculated at $\xi = 0.025$ may be considered as a recommended value for calculations within the flame. Thus an almost spatially constant value of λ_{rz} of 0.065 was found. However, there was a slight downward trend with swirl.

CONCLUSION

A method is presented[2] which allows the distributions of the significant flux components [τ_{rz} , $\tau_{r\theta}$, $(J_h)_r$ and $(J_j)_r$] and associated exchange coefficients, Prandtl and Schmidt numbers to be determined from experimental time-mean distributions

[2] Complete numerical, computational, and program details are available in [1, 4].

of v_z, v_θ, T and m_j. It thus provides a link between mean measurements and certain correlations of turbulent fluctuation components and throws light on the appropriateness or otherwise of any given turbulence model for the flow under consideration. The method is applied to both isothermal and chemically reacting flows, and calculations show that previous isotropy and constant Prandtl–Schmidt number assumptions are not generally valid and that the turbulent stress distribution is nonisotropic. The exchange coefficients are shown to be functions of the degree of swirl and position in the flowfield. For the isothermal case it is shown that the assumption of an isotropic uniform mixing length parameter distribution is quite feasible for weak swirl but is progressively less valid as the degree of swirl increases. For the flame case, similar results are obtained and the turbulent viscosity is found to be highly nonisotropic.

REFERENCES

1. D. G. LILLEY AND N. A. CHIGIER, "TEXCO: A Turbulent Flux and Exchange Coefficient Code for Nonrecirculating Swirling Combustion Systems using Mean Value Distributions," Report No. FTCE/13/DGL/5/70, Dept. of Fuel Tech. and Chem. Eng., Sheffield Univ., Sheffield, England, 1970.
2. D. G. LILLEY AND N. A. CHIGIER, Nonisotropic turbulent stress distribution in swirling flows from mean value distributions, *Int. J. Heat Mass Transfer* **14** (1971), 573–585.
3. D. G. LILLEY AND N. A. CHIGIER, Nonisotropic Exchange Coefficients in Turbulent Swirling Flames from Mean Value Distributions," Presented at the Thirteenth International Symposium on Combustion, Salt Lake City, Utah, 1970; *Combustion and Flame*, **16** (1971), 177–189.
4. D. G. LILLEY, "Theoretical Study of Turbulent Swirling Boundary Layer Flow with Combustion," Ph.D. Thesis, Dept. of Chemical Eng. and Fuel Tech., Sheffield University, Sheffield, England, 1970.
5. L. PRANDTL, Bericht über Untersuchungen zur ausgebildeten Turbulenz, *ZAMM* **5** (1925), 136.
6. N. P. L., "Modern Computing Methods," 2nd. ed., Notes on Applied Science Series No. 16, Her Majesty's Stationery Office, London, 1961.
7. N. A. CHIGIER AND A. CHERVINSKY, Experimental investigation of swirling vortex motion in jets, *J. Appl. Mech.* **34** (1967), 443–451.
8. S. V. PATANKAR AND D. B. SPALDING, A finite-difference procedure for solving the equations of the two-dimensional boundary layer, *Int. J. Heat Mass Transfer* **10** (1967), 1389–1411.
9. W. R. HAWTHORNE, D. S. WEDDELL, AND H. C. HOTTELL, "Proceedings of the Third International Symposium on Combustion, Flame and Explosion Phenomena," p. 266, Williams and Wilkins, Baltimore, MD, 1949.
10. N. A. CHIGIER AND A. CHERVINSKY, "Aerodynamic Study of Turbulent Burning Free Jets with Swirl," p. 489, Eleventh International Symposium on Combustion, The Combustion Institute, Pittsburgh, PA, 1967.